

# Active earth pressure with consideration of displacement effect of retaining wall<sup>1</sup>

JICAI LI<sup>2,3</sup>, BOWEN YU<sup>4</sup>, JINGBO SU<sup>5</sup>

**Abstract.** The existing problems of the calculation theory and method of earth pressure are analyzed and discussed. Based on the theory of soil arching, the stress state and the effect of principal stress rotation of backfill behind the wall are analyzed. Further, a new computation method for the earth pressure which considers the displacement effect of the retaining wall is obtained. The distribution of earth pressure of retaining wall is gained for the displacement mode of translation motion, rotation about the top and rotation about the bottom. And the change of the joint force and its position of earth pressure is analyzed along with the change of displacement value. Comparison is made among the results calculated by the proposed method, the other methods and the test observations. It can be demonstrated that the calculating results by the proposed method have better agreement with those of the experimental observations.

**Key words.** Displacement mode, theory of soil arching, distribution of earth pressure, active earth pressure, retaining wall.

## 1. Introduction

Retaining wall is one of the most widely-used retaining structures. Correspondingly, how to calculate earth pressure reasonably and accurately and to ensure its security and stability is an important topic for many scholars. The classical theory of earth pressure is widely used in many engineering designs. However, Terzaghi found the earth pressure behind the wall is not linear by different model experiments in 1943, what is more, the slip crack surface in classical theory is questioned by many

---

<sup>1</sup>Majority of the work presented in this paper was funded by the National Natural Science Foundation of China (Grant No. 51679081).

<sup>2</sup>Nanjing Hydraulic Research Institute, Nanjing, Jiangsu, 210029, China

<sup>3</sup>Nanjing R&D Tech Group co., LTD., Nanjing, Jiangsu, 211106, China

<sup>4</sup>School of Hydraulic Engineering, Dalian University of Technology, Dalian, Liaoning, 116024, China

<sup>5</sup>College of Harbour, Coastal and Offshore Engineering, Hohai University, Nanjing, Jiangsu, 210098, China

scholars [1], and the slip crack surface is a curved surface which was verified by many model and field experiment.

The earth pressure behind the wall has been proved to be nonlinear distribution by different model experiments by Fang and Ishibashi [2]. Also, it can be found that the earth pressure has different distributions for different displacement pattern and size. The earth pressure behind the retaining wall is closely related to the displacement effect of retaining wall. Many methods such as theoretical analysis [3], numerical simulation [4] and model experiment [5] are used to research the distribution of earth pressure behind the wall.

However, there are some insufficiencies about the research methods. First of all, the plain slip crack surface is used in many researches [6], the defect of the classical theory cannot be escaped. Although other researches [7], [8] partly consider that the slip crack surface is nonlinear, the slip crack surface was artificially supposed by simple curve equation. Secondly, there are some problems with the assumption of the trajectory and top surface of soil arch, and the non-uniform distribution and non-uniform change of compression stress in horizontal soil element do not considered, that cannot reflect the real situations. Finally, many studies [9] can only be used when the soil behind the wall reached fully active state, and that cannot consider the effect of the wall displacement pattern and the size of displacement for the size and distribution of earth pressure at the same time.

In this paper, the existing problems of the calculation theory and method of earth pressure are analyzed and discussed. A new computation method for the earth pressure which considers the displacement effect of the retaining wall is obtained by the theory of soil arching, the stress state and the effect of principal stress rotation of backfill behind the wall.

## 2. Methodology

### 2.1. Assumption of soil arching effect

If a retaining wall deforms outward, and the displacement is big enough, the soil behind the wall will be destroyed along the slip crack surface. The soil will be subjected to shear stresses from slip surface and contact surface of soil and wall. At this time, the direction of principal stress will rotate and the track of minor primary stress is a bending curve. The track of minor principal stress is assumed as a circular arch in this paper. In any depth, the radius  $r$  of soil arch is

$$r = \frac{L}{(\cos \beta_w - \cos \beta_s)}, \quad (1)$$

where  $L$  is the length of horizontal layer element,  $\beta$  is the angle between the third principal stress and horizontal direction,  $\beta_w$  is the angle between the third principal stress and the horizontal direction at the retaining wall, and  $\beta_s$  is the angle between the third principal stress and the horizontal direction at the slip crack surface.

The calculation model is shown in Fig. 1. The wall is a rigid body, its back is



As the wall deflects from soil to a certain extent, the soil behind the wall will reach the fully active condition. At this time, the soil will be forced by friction from the wall surface and the slip crack surface, and the principal stress rotation will happen, where the stress state is shown in Fig. 2 and Fig. 3.

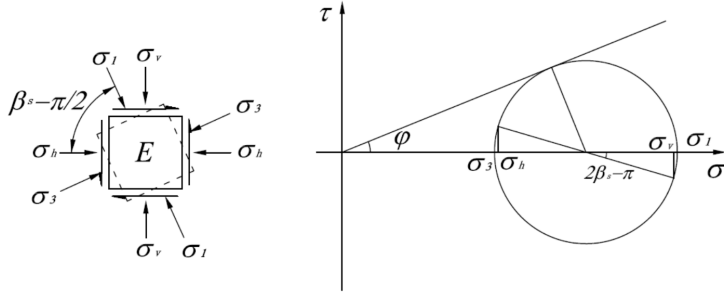


Fig. 3. Stress state at point E

For point D, the angle between the third principal stress and horizontal direction is

$$\beta_w = \tan^{-1} \left[ \frac{N - 1 \pm \sqrt{(N - 1)^2 - 4N \tan^2 \delta}}{2 \tan \delta} \right]. \quad (2)$$

and for the point E we get

$$\beta_s = \alpha + \frac{\pi}{4} - \frac{\varphi}{2}. \quad (3)$$

In the above formulas

$$N = \frac{\sigma_1}{\sigma_3} = \tan^2 \left( \frac{\pi}{4} + \frac{\varphi}{2} \right)$$

is the ratio between the major principal stress  $\sigma_1$  and minor principal stress  $\sigma_3$  and  $\alpha$  is the angle between slip crack surface and horizontal direction.

From Eq. (3), if  $\alpha > \varphi/2 + \pi/4$ , then  $\beta_s > \pi/2$ , and we can see that the rotation directions of the principal stress at the slip crack surface and the wall surface are opposite. If  $\alpha < \varphi/2 + \pi/4$ , then  $\beta_s < \pi/2$ , and we can see that the rotation directions of the principal stress at the slip crack surface and the wall surface are the same. The rotation angles of the principal stress at the slip crack surface change with the depth. The change reflects the slide surface is nonlinear. That is to say, the slide surface is a curved surface with the changing angle  $\alpha$ .

By the stress analysis, we know that the horizontal stress of point in each slice is

$$\sigma_h = \sigma_1 \cos^2 \beta + \sigma_3 \sin^2 \beta, \quad (4)$$

the vertical stress is

$$\sigma_v = \sigma_1 \sin^2 \beta + \sigma_3 \cos^2 \beta, \quad (5)$$

and the shear stress is

$$\tau = (\sigma_h - \sigma_3) \tan \beta, \quad (6)$$

where  $\beta$  is the angle between the third principal stress and horizontal direction at the given point.

The length of each slice behind the wall can be obtained as

$$L = r(\cos \beta_w - \cos \beta_s). \quad (7)$$

For the differentiation element of each slice we can get the width of the differentiation element

$$dL = r \cdot \sin \beta d\beta. \quad (8)$$

Considering the principal stress rotation behind the wall, the average vertical force on each slice is obtained by the following formula

$$\bar{\sigma}_v = \frac{1}{L} \int_{\beta_w}^{\beta_s} \sigma_v dL = \frac{1}{L} \int_{\beta_w}^{\beta_s} \sigma_1 \left( \sin^2 \beta + \frac{\cos^2 \beta}{N} \right) \cdot r \cdot \sin \beta d\beta. \quad (9)$$

Substitution of Eq. (9) yields

$$\bar{\sigma}_v = A\sigma_1, \quad (10)$$

where

$$A = \frac{1}{(\cos \beta_w - \cos \beta_s)} \left[ (\cos \beta_w - \cos \beta_s) - \frac{1 - 1/N}{3} (\cos^3 \beta_w - \cos^3 \beta_s) \right]. \quad (11)$$

In this way we can obtain the coefficient of active earth pressure

$$K = \frac{\sigma_{dh}}{\bar{\sigma}_v} = \frac{\cos^2 \beta + \frac{\sin^2 \beta}{N}}{A}. \quad (12)$$

## 2.2. The calculation method of active earth pressure

If the displacement of the wall away from the fill takes place, the load-bearing state of each slice is shown in Fig. 1. By the equilibrium condition, the vertical stress is

$$\bar{\sigma}_{vi+1} = \frac{(L_i - \frac{B_i}{A_i} \Delta y) \bar{\sigma}_{vi} + \Delta G}{L_{i+1} + \frac{B_{i+1}}{A_{i+1}} \Delta y}, \quad (13)$$

where

$$A_i = \frac{1}{(\cos \beta_{wi} - \cos \beta_{si})} \left[ (\cos \beta_{wi} - \cos \beta_{si}) - \frac{1 - 1/N}{3} (\cos^3 \beta_{wi} - \cos^3 \beta_{si}) \right], \quad (14)$$

$$B_i = \frac{1}{2} (\cos^2 \beta_{wi} + \frac{\sin^2 \beta_{si}}{N}) \tan \delta + \frac{(1 - 1/N) \cos \varphi \cos(\alpha_i - \varphi)}{4 \sin \varphi \sin \alpha_i}. \quad (15)$$

The active earth pressure in horizon against the retaining wall can be expressed as

$$p_{xi} = \sigma_{dh} = \frac{\cos^2 \beta + \frac{\sin^2 \beta}{N}}{A} \bar{\sigma}_{vi+1}. \quad (16)$$

The resultant force of active earth pressure at horizontal direction is

$$P_{xi} = \sum \frac{(p_{xi} + p_{xi+1})}{2} \Delta y, \quad (17)$$

and its location

$$h_P = \frac{\sum 0.5(p_{xi} + p_{xi+1}) \cdot \Delta y (H - y_i - 0.5\Delta y)}{Q_x}, \quad (18)$$

where  $Q_x$  is the resultant force of horizontal earth pressure.

### 2.3. The displacement effect

It is very important for the size and distribution of active earth pressure whether the soil achieves the active state. In order to achieve fully active state of the soil, the friction angle of the interface between wall and soil must be fully working. The definition of active state is more strictly for the non-limit state of soil, the friction angle of the interface between wall and soil must be also fully working [10]. So the working state of the internal friction angle  $\varphi$  of the backfill and friction angle  $\delta$  of the interface between wall and soil are related to the displacement of the backfill. By the analysis of the working state of  $\varphi$  and  $\delta$ , the progressive failure process of the backfill can be simulated and the size and distribution of active earth pressure can be computed.

In this paper, we take the Chang's model to match the working state of  $\varphi$  and  $\delta$  by  $\varphi_m$  and  $\delta_m$  (where  $\varphi_m$  and  $\delta_m$  are, respectively, the internal friction angle of the soil in the Chang's model and the friction angle of the contact surface on the wall in the Chang's model). The relationship between the friction angle and displacement is illustrated in Fig. 4.

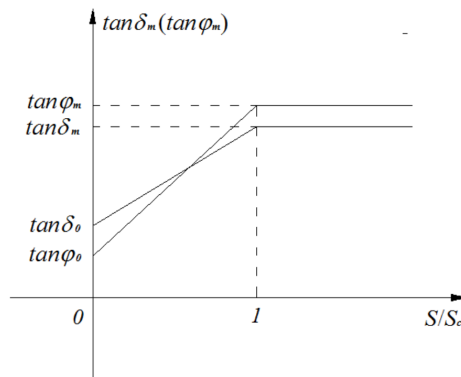


Fig. 4. Relationship between friction angle and displacement

While the retaining wall deforms outwards, the relationship between the friction

angle and displacement can be described as

$$\tan \varphi = \tan \varphi_0 + (\tan \varphi_m - \tan \varphi_0) \frac{S}{S_c}, \quad (19)$$

$$\tan \delta = \tan \delta_0 + (\tan \delta_m - \tan \delta_0) \frac{S}{S_c}, \quad (20)$$

where  $\varphi_0$  and  $\delta_0$  are the initial values of internal friction angle of the backfill and friction angle of the interface between wall and soil respectively; its value may refer to Chang's thesis. Symbol  $S$  is the soil displacement of the calculation point, while  $S_c$  is the soil displacement of calculation point when the soil achieves fully active state.

According to the model test of Fang and Ishibashi, each point of the soil reaches active state needs the same displacement along the retaining wall. Furthermore, the displacement is independent of the wall displacement pattern. Thus, we assume that the translational displacement  $S_a$  is  $0.0005H$  when the soil achieves active state, the rotation angles about the top and the bottom are respectively  $0.0015$  rad and  $0.001$  rad when the soil achieves active state.

In this paper, the Fang and Ishibashi's experiment is taken as the calculation example for the comparisons and analysis. In the experiment, the surface of the retaining wall is vertical, the height of the wall is  $1$  m, the backfill behind the retaining wall is sandy soil whose unit weight  $\gamma = 15.4 \text{ kN/m}^3$  and the internal friction angle  $\varphi = 34^\circ$ . In the calculation, the friction angle between soil and wall  $\delta = 2\varphi/3 = 22.67^\circ$ , the initial value of internal friction angle of the backfill  $\varphi_0 = 9.69^\circ$ , the friction angle of the interface between wall and soil  $\delta_0 = 4.16^\circ$ .

### 3. Result analysis and discussion

#### 3.1. The slip crack surface

Different from the Coulomb theory, the angle is greater than the angle of the Coulomb's classical slip crack surface, and the width on the top of the slip crack surface is smaller for the displacement pattern of translational motion (T mode). For the displacement pattern of rotation about the bottom (RB mode), the angle between the slip crack surface and the horizontal direction decreases with the increasing depth by a smooth curved surface, the slip crack surface is steeper than the Coulomb's classical slip crack surface at the upper of the retaining wall and flatter than the Coulomb's classical slip crack surface at the bottom of the retaining wall. The width on the top of the slip crack surface is wider than that of the displacement pattern of translational motion, narrower than that of the Coulomb's theory. For the displacement pattern of rotation about the top (RT mode), at the upper of the retaining wall, the slip crack surface is a potential slip crack surface and it is flatter than the Coulomb's classical slip crack surface. At the lower of the retaining wall, the slip crack surface is steeper than the Coulomb's classical slip crack surface, the width on the top of the slip crack surface is wider than that of the displacement

pattern of translational motion, narrower than that of the Coulomb's theory. The shape of the slip crack surface is shown in Fig. 5.

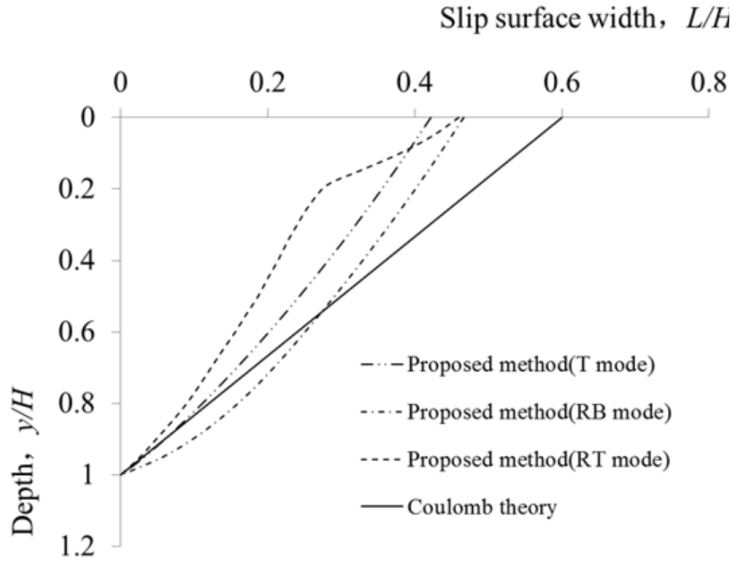


Fig. 5. Shape of slip crack surface

### 3.2. The earth pressure distribution

For the displacement pattern of translational motion (T mode), the active earth pressure increases with the increasing of depth at the upper and middle of the retaining wall, but the increasing rate decreases. The active earth pressure decreases with the increasing of depth at the bottom of the retaining wall. For the displacement pattern of rotation about the bottom (RB mode), the active earth pressure is same with that of T mode at the upper of the retaining wall because of the fully active state of the backfill; at the lower of the retaining wall, the backfill does not reach fully active state because of the smaller displacement, so the active earth pressure is bigger than that of T mode; at the bottom of the retaining wall, the active earth pressure is obviously larger than that of the Coulomb's theory. For the displacement pattern of rotation about the top (RT mode), the earth pressure is large because of the shear stress from the lower soil and the frictional force from the wall at the upper of the retaining wall; at the lower of the retaining wall, the active earth pressure increases firstly, then decreases with the increasing depth because of the fully active state of the backfill. Compared with the model test and Coulomb theory, the calculation method in this paper can reflect obviously the change rules of the active earth pressure, especially at the bottom of the wall, as is shown in Fig. 6.



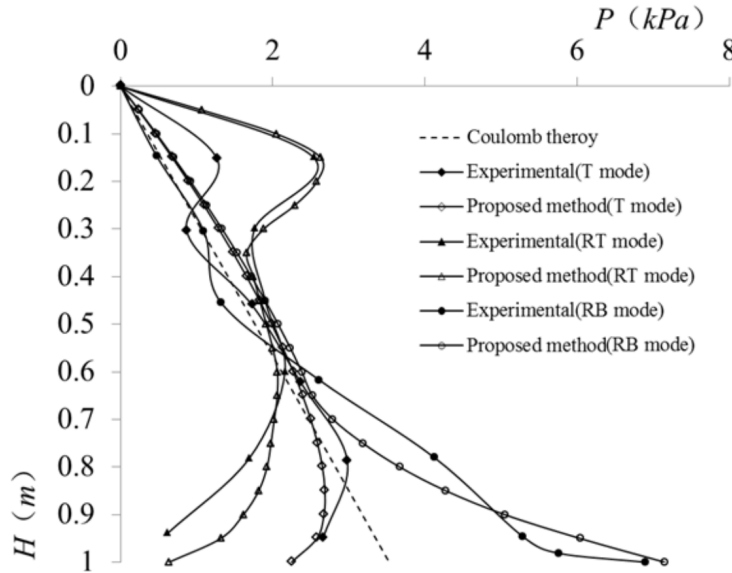


Fig. 6. Earth pressure distribution

### 3.3. The resultant force

The resultant force of active earth pressure decreases with the increasing of displacement and the decreasing rate decreases under different displacement of retaining wall. For the displacement pattern of translational motion (T mode), the location of the resultant force is higher than  $H/3$  by Coulomb's theory, while the location of the resultant force of active earth pressure is about  $H/3$  with the displacement pattern of rotation about the top (RT mode) and higher than  $H/3$  with displacement pattern of rotation about the top (RT mode), as is shown in Fig. 7 and in Fig. 8.

## 4. Conclusion

In this paper, according to the analysis of the stress state and the effect of principal stress rotation of backfill behind the wall, the calculation method for active earth pressure which considers the effect of displacement of the retaining wall is established. Also, the obtained results of active earth pressure have good agreement with the test results.

The distribution curves of active earth pressure are nonlinear: for the T mode, the active earth pressure increases with the increasing of depth at the upper and middle of the retaining wall, the active earth pressure decreases with the increasing of depth at the bottom of the retaining wall; for the RB mode, the active earth pressure is same with that of T mode at the upper of the retaining wall, the active earth pressure is bigger than that of T mode or the Coulomb's theory at the lower of

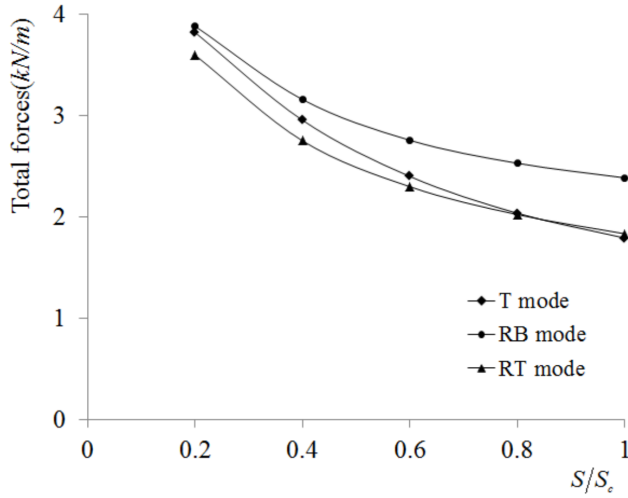


Fig. 7. Curve of the resultant force

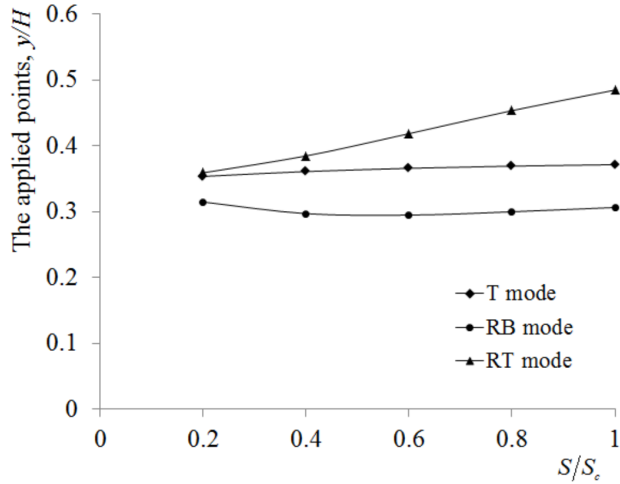


Fig. 8. Curve of the resultant force

the retaining wall; for the RT mode, the active earth pressure is large at the upper of the retaining wall, the active earth pressure increases firstly, then decreases with the increasing depth.

The resultant force of active earth pressure decreases with the increasing of displacement for three displacement modes: T mode, RB mode, and RT mode. For the T mode, the location of the resultant force of active earth pressure is higher than  $H/3$  by Coulomb's theory; for the RB mode, the location of the resultant force of active earth pressure is about  $H/3$ ; for the RT mode, the location of the resultant force of active earth pressure increases with the increasing displacement of rotation

and is higher than  $H/3$ .

## References

- [1] L. CHEN: *Active earth pressure of retaining wall considering wall movement*. European Journal of Environmental and Civil Engineering 18 (2014), No. 8, 910–926.
- [2] Y. S. FANG, I. ISHIBASHI: *Static earth pressures with various wall movements*. Journal of Geotechnical Engineering 112 (1986), No. 3, 317–333.
- [3] M. H. KHOSRAVI, T. PIPATPONGSA, J. TAKEMURA: *Theoretical analysis of earth pressure against rigid retaining walls under translation mode*. Soils and Foundations 56 (2016), No. 4, 664–675.
- [4] O. RAHMOUNI, A. MABROUKI, D. BENMEDDOUR, M. MELLAS: *A numerical investigation into the behavior of geosynthetic-reinforced soil segmental retaining walls*. International Journal of Geotechnical Engineering 10 (2016), No. 5, 435–444.
- [5] M. F. CHANG: *Lateral earth pressures behind rotating walls*. Canadian Geotechnical Journal 34 (1997), No. 4, 498–509.
- [6] P. RAO, Q. CHEN, Y. ZHOU, S. NIMBALKAR: *Determination of active earth pressure on rigid retaining wall considering arching effect in cohesive backfill soil*. International Journal of Geomechanics 16 (2016) No. 3, 04015082.
- [7] W. KUIHUA, M. SHAOJUN, W. WENBING: *Active earth pressure of cohesive soil backfill on retaining wall with curved sliding surface*. Journal Southwest Jiaotong University 46 (2011), No. 5, 732–738.
- [8] E. LEVENBERG, N. GARG: *Estimating the coefficient of at-rest earth pressure in granular pavement layers*. Transportation Geotechnics 1 (2014), No. 1, 21–30.
- [9] Y. T. ZHOU, Q. S. CHEN, F. Q. CHEN, X. H. XUE, S. BASACK: *Active earth pressure on translating rigid retaining structures considering soil arching effect*. European Journal of Environmental and Civil Engineering (2016), 1–17.
- [10] M. A. SHERIF, I. ISHIBASHI, C. D. LEE: *Earth pressures against rigid retaining walls*. Journal of the Geotechnical Engineering Division 108, (1982), No. 5, 679–695.

Received April 23, 2017

